Diblock Copolymer Nanospheres with Porous Cores

Jiayun Zhou, Zhao Li, and Guojun Liu*

Department of Chemistry, University of Calgary, 2500 University Dr., NW, Calgary, Alberta, Canada T2N 1N4

Received November 16, 2001; Revised Manuscript Received February 4, 2002

ABSTRACT: Nanospheres with porous cores were prepared from a diblock copolymer poly[(2-cinnamoyloxyethyl methacrylate)-*random*-(2-(1′-thyminylacetoxyethyl methacrylate)]-*block*-poly(*tert*-butyl acrylate), P(CEMA-*r*-T)-*b*-P*t*BA, where the CEMA groups are photo-cross-linkable and the thyminyl groups can H bond with adenine. When mixed with poly[(2-hydrocinnamoyloxyethyl methacrylate)-*random*-2-(9′-adeninylacetoxyethyl methacrylate) or P(hCEMA-*r*-A), P(CEMA-*r*-T)-*b*-P*t*BA formed micelles in chloroform/cyclohexane (CHX) with P*t*BA coronas and cores consisting of P(CEMA-*r*-T) and P(hCEMA-*r*-A). Pores were generated after photo-cross-linking the cores and extracting out the porogen P(hCEMA-*r*-A) with DMF. The presence of pores in the cores of the nanospheres was demonstrated by the much faster uptake of adenine from methanol by the porous nanospheres than the solid nanospheres prepared from P(CEMA-*r*-T)-*b*-P*t*BA without using the porogen. This was also confirmed by the much higher capacity of the porous nanospheres for P(hCEMA-*r*-A) uptaking.

I. Introduction

Pores in cross-linked polymer resins are generated from removing entrapped porogens to enhance reagent transport and to increase internal pore volume and surface areas.[1] Porogen can be a saturated polymer or a solvent or nonsolvent for the polymer matrix to be cross-linked. Use of a nonsolvent leads to polymer and nonsolvent phase separation during polymerization and the evaporation of the nonsolvent after polymer formation yields macropores with sizes larger than ∼2 nm. Use of a solvent during polymer preparation leads to the production of micropores with sizes below ∼2 nm. Much larger macropores, >50 nm, are produced from the use of polymeric porogens after their extraction from cross-linked polymer resins.

Pores can also be produced with their shapes matching those of the templating molecules from the molecular imprinting technique.[2] In this case, the degree of cross-linking is high so that the configuration of the templating molecule and those of the binding groups of the matrix are locked in. The cavities with the binding groups on the walls after template removal would bind selectively with analytes that possess similar shapes and binding configurations as the template. Molecularly imprinted polymer resins have been used to separate racemic isomers,[3] nucleotide bases,[4,5] metal ions,[6] and biopolymers[7,8] etc.

Pores have been produced mainly in bulk polymers,[2] micrometer-sized beads[9−11] or monolithic rod columns.[12,13] Reported here is the generation of pores in the cross-linked cores of diblock copolymer nanospheres. The preparation involved dissolving the diblock poly[(2-cinnamoyloxyethyl methacrylate)-*random*-(2-(1′-thyminylacetoxyethyl methacrylate)]-*block*-poly(*tert*-butyl acrylate) or P(CEMA-*r*-T)-*b*-P*t*BA and the porogen poly[(2-hydrocinnamoyloxyethyl methacrylate)-*random*-2-(1′-adeninylacetoxyethyl methacrylate) or P(hCEMA-*r*-A) in chloroform first. The adenine groups (A) of P(hCEMA-*r*-A) and the thymine groups (T) of P(CEMA-*r*-T)-*b*-P*t*BA were probably H bonded at this stage (Scheme 1). Addition of CHX, which solubilized P*t*BA only, led to formation of micelles consisting of P(CEMA-*r*-T) and P(hCEMA-*r*-A) cores and P*t*BA coronas. The structure of the cores was then locked in from photo-cross-linking the PCEMA. Nanospheres with porous cores were obtained after extracting out P(hCEMA-*r*-A). Also reported in this paper is the recognition or selective uptake of P(hCEMA-*r*-A) by the porous nanospheres from chloroform.

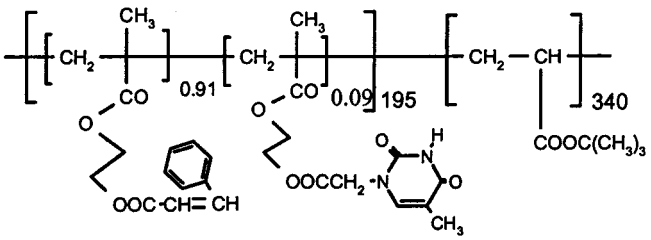

P(CEMA-*r*-T)-*b*-P*t*BA

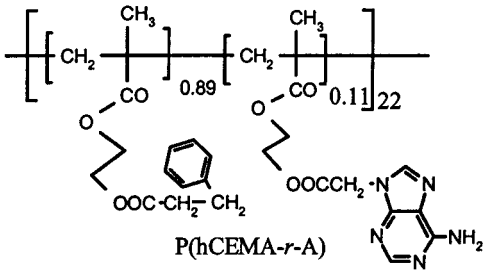

P(hCEMA-*r*-A)

Although H bonding has been used to induce polymer micelle formation,[14] it has not been used to facilitate porogen introduction into the cores of block copolymer micells. We have used an oligomer as porogen to produce diblock nanospheres with porous cores before.[15] Due to the lack of specific binding between the porogen and the core block used, the nanospheres produced probably lacked molecular recognition capability. In addition to porous nanospheres prepared from this approach, other similar nanostructures would include block copolymer vesicles,[16−19] cross-linked vesicles,[20] and nanospheres with hollow cores generated from core block degradation.[21]

10.1021/ma0120005 CCC: $22.00
Published on Web 03/19/2002

Scheme 1

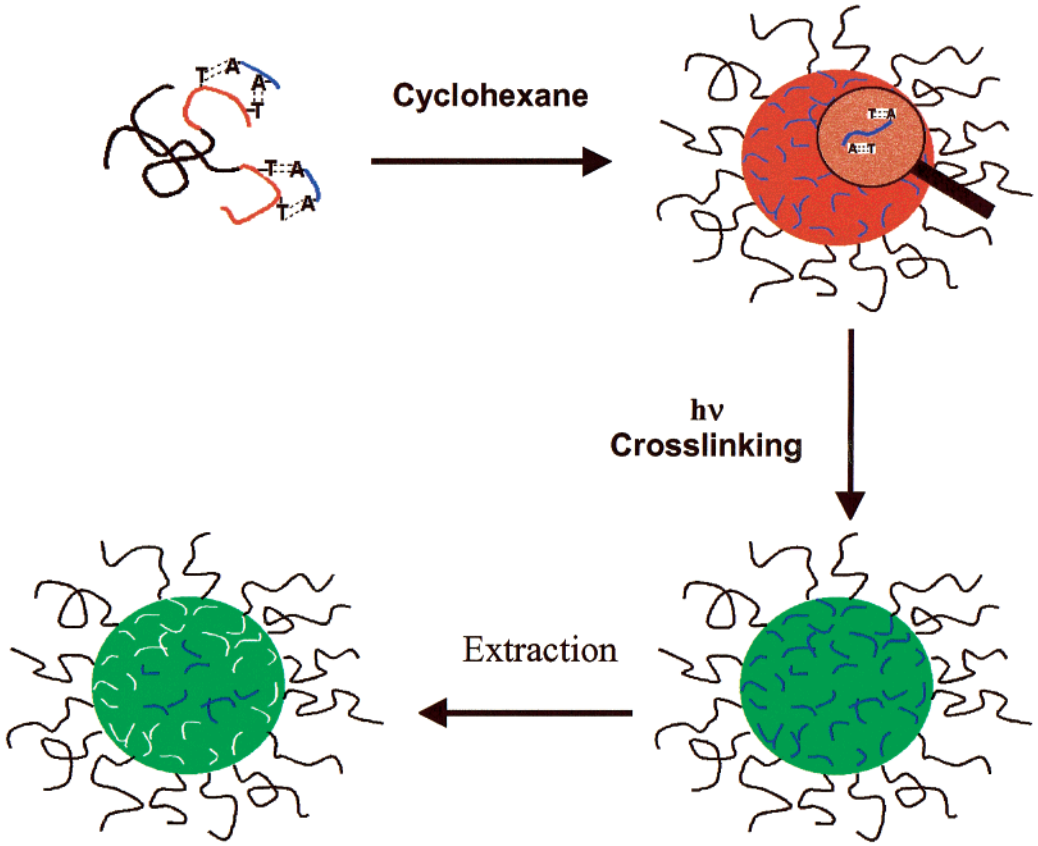

II. Experimental Section

Synthesis and Characterization of PHEMA-*b*-P*t*BA and PHEMA. One precursory diblock copolymer P(HEMA-TMS)-*b*-P*t*BA and a P(HEMA-TMS) oligomer were synthesized by anionic polymerization for this project, where P(HEMA-TMS) denotes poly(2-trimethylsiloxylethyl methacrylate). The procedures used to purify the monomers, to perform the polymerizations and to isolate the polymers have been detailed before[22] and are therefore not repeated here. P(HEMA-TMS)-*b*-P*t*BA thus synthesized was hydrolyzed in THF/methanol (v/v = 20/80) overnight to yield PHEMA-*b*-P*t*BA, where PHEMA denotes poly(2-hydroxylethyl methacrylate). For sample characterization, the PHEMA-*b*-P*t*BA sample was made soluble in common organic solvents such as THF and chloroform by reacting with cinnamoyl chloride to yield PCEMA-*b*-P*t*BA, where PCEMA denotes poly(2-cinnamoyloxyethyl methacrylate). The PHEMA block was converted into a PCEMA block, as the esterification step had been utilized extensively in our laboratory. The PCEMA-*b*-P*t*BA diblock was characterized by gel permeation chromatography, light scattering, and NMR, following procedures detailed before.[23] The targeted number of repeat units for the PHEMA oligomer was 25.

P(HEMA-*r*-T)-*b*-P*t*BA. The PHEMA block of PHEMA-*b*-P*t*BA was tagged with thymine groups from reacting with 1-thymine acetic acid (Aldrich, 98%). In a sample run, PHEMA-*b*-P*t*BA, 0.3045 g containing 0.862 mmol of hydroxyl groups, 1-thymine acetic acid, 0.0523 g or 0.234 mmol, and catalyst 4-(dimethylamino)pyridine,[24] 0.0037 g or 0.030 mmol, were dissolved in 10 mL of dry *N*,*N*-dimethylformamide (DMF). The mixture was cooled to 0 °C in an ice bath before dicyclohexyl carbodiimide (DCC), 0.0878 g or 0.486 mmol, was added. After reaction overnight, the product was purified by dialysis against methanol changed six times over 2 days in a tube with a molar mass cutoff between 12 000 and 14 000 g/mol. After methanol evaporation, P(HEMA-*r*-T)-*b*-P*t*BA, 0.3012 g, was obtained as a white solid.

P(CEMA-*r*-T)-*b*-P*t*BA. P(HEMA-*r*-T)-*b*-P*t*BA, 0.300 g, and cinnamoyl chloride (Aldrich, 98%), 0.4279 g or 2.50 mmol, were dissolved in 10 mL of dry pyridine. The mixture was stirred overnight before the salt formed was filtered and the supernatant was added on ice to precipitate out the polymer. After vacuum-drying, 0.4015 g of white P(CEMA-*r*-T)-*b*-P*t*BA solid was obtained.

6-*N*-(Benzyloxycarbonyl)-9-(carboxymethyl)adenine or Compound 1. Procedures used to synthesize and characterize this compound were detailed in the original literature[25] and are not repeated here. The reactions involved are

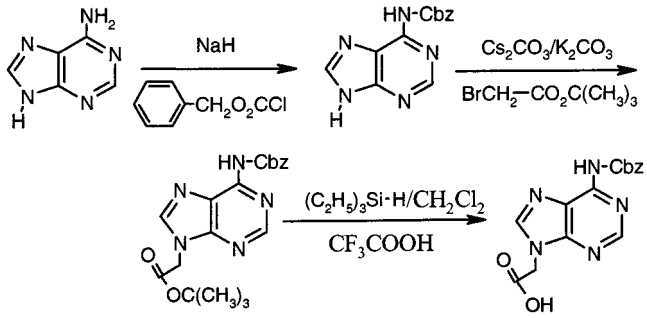

where adenine (99%), benzyl chloroformate (95%), *tert*-butyl-bromoacetate (98%), triethylsilane (95%), and trifluoroacetic acid (TFA, 99+%) were all purchased from Aldrich and used as received.

P(HEMA-*r*-1). Compound **1** was attached to the PHEMA oligomer via esterification between the carboxyl groups of **1** with the hydroxyl groups of PHEMA. PHEMA, 0.35 g containing 2.7×10^{-3} mol of hydroxyl groups, and **1**, 0.26 g or 0.80×10^{-3} mol, were dissolved in dry pyridine. Then added were the catalyst *p*-toluenesulfonic acid,[26] 0.0153 g or 0.080 mmol, and DCC, 0.1651 g or 0.80 mmol. The mixture was stirred at room temperature for 2 days before it was dialyzed against methanol changed six times over 2 days in a tube with a molar mass cutoff of 1000 g/mol. After solvent evaporation, P(HEMA-*r*-**1**), 0.38 g, was obtained.

PhCEMA and P(hCEMA-*r*-A). The procedures used to produce PhCEMA or P(hCEMA-*r*-**1**) were very similar to those of P(CEMA-*r*-T)-*b*-P*t*BA synthesis. Here, hydrocinnamoyl chloride (Aldrich, 98%) and PHEMA or P(HEMA-*r*-**1**) were used as the starting materials. To cleave the benzylcarbonyl protective group of the 9-amino group of adenine, P(hCEMA-*r*-**1**) was dissolved in neat TFA and heated at 80 °C for 2 h. TFA was then evaporated by vacuum distillation and the remaining volatiles were removed by azeotroping with chloroform three times to give a solid product.

Micelle Formation, Cross-linking, and Porous Nanosphere Preparation. P(CEMA-*r*-T)-*b*-P*t*BA, 0.2415 g containing 4.5×10^{-5} mol of thymine groups, and P(hCEMA-*r*-A), 0.0237 g containing 1.0×10^{-5} mol of adenine groups, were dissolved in 75 mL chloroform. After the mixture was stirred overnight, CHX, 188 mL, was added. The micelles formed were further equilibrated at 60 °C overnight before irradiation with a focused light beam from a 500-W Hg lamp passed a 290 nm cutoff filter. The PCEMA double bond conversion measured from absorbance decrease at 274 nm was 36%.[23]

Porous nanospheres were produced after extracting out the porogen with DMF. The cross-linked nanospheres, 200 mg, were dialyzed against DMF that was changed a total of five times over 3 days, in a tube with a molar mass cutoff of 50 000 g/mol. After the solution collected outside the dialysis tube was dried, 16 mg of solid was obtained. A ^{1}H NMR analysis indicated that the extracted polymer was exclusively P(hCEMA-*r*-A). A comparison with the initial porogen loading of 0.0981 g/g gave a porogen recovery efficiency of 90% for this sample.

PCEMA-*b*-P*t*BA and P(CEMA-*r*-T)-*b*-P*t*BA micelles and nanospheres were prepared similarly without using the porogen P(hCEMA-*r*-A) and an extraction step. The PCEMA double bond conversions for these two samples were 38% and 37%, respectively.

Adenine Uptake. Nanospheres, 5.0 mg, dissolved in 5.0 mL of methanol were dispensed into a dialysis tube with a molar mass cutoff of 12 000−14 000 g/mol. The tube was then inserted into 100 mL of a stirred 2.3-ppm adenine solution in methanol. Then 1.00 mL of sample was taken at predesignated times outside the tube and diluted for adenine absorbance analysis at 260 nm. To correct for adenine dilution by methanol inside and sorption by the dialysis tube, a control experiment was performed. In this case, no nanospheres but only 5.00 mL of methanol was initially dispensed into the tube.

P(hCEMA-*r*-A) and PCEMA Uptake. The experiments were performed similarly as described above except that the solvent used here was chloroform. Also, the initial adsorbate P(hCEMA-*r*-A) or PCEMA concentration used was 60 ppm rather than 2.3 ppm. P(hCEMA-*r*-A) and PCEMA concentration changes were followed from absorbance decreases at 260 and 274 nm, respectively.

Dynamic Light Scattering and TEM Measurements. Nanosphere or micellar solutions at ~0.1 mg/mL in chloroform/CHX (v/v = 1/2.5) were used for dynamic light scattering studies (DLS) at a scattering angle of 90°. The samples were clarified by passing them through 0.2 μm filters. The viscosity of the solvent mixture was estimated from the sum of the individual components' values each multiplied by its volume fraction. A similar relation was used to estimate the refractive index of the mixture. The instrument used was of a Brookhaven model 9025 equipped with a He−Ne laser operated at 632.8 nm.

A Hitachi-7000 instrument was operated at 75 kV to obtain the transmission electron microscopy (TEM) images of the micelles and nanospheres. All samples were aspirated from chloroform/CHX at v/v = 1/2.5, using a home-built device as described before,[27] and stained with OsO_4 vapor.

III. Results and Discussion

Polymer Synthesis and Characterization. Many compounds and polymers were prepared and the two key polymers were P(CEMA-*r*-T)-*b*-P*t*BA and P(hCEMA-*r*-A). GPC polydispersity and number-average molar mass, $\bar{M}_n$, of P(hCEMA-*r*-A) against PMMA standards were 1.36 and 5800 g/mol, respectively. The $\bar{M}_n$ value corresponded to an average repeat unit number of ~22, which was in good agreement with the targeted value of 25. Shown in Figure 1a is a ^{1}H NMR spectrum of the P(hCEMA-*r*-A) sample. Also shown in Figure 1 are peak assignments for P(hCEMA-*r*-A) and P(CEMA-*r*-T)-*b*-P*t*BA. From the intensity ratio of a peak at 8.5 ppm for adenine and that at 2.6 ppm for hCEMA, an adenine labeling efficiency of 11% was obtained.

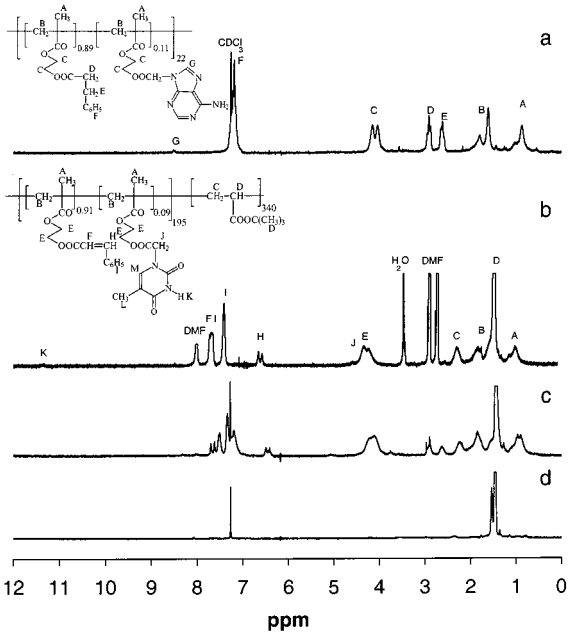

Figure 1. ^{1}H NMR spectra of P(hCEMA-*r*-A) in $CDCl_3$ (a), P(CEMA-*r*-T)-*b*-P*t*BA in DMF-d_6 (b), a mixture of P(CEMA-*r*-T)-*b*-P*t*BA, 5.2 mg, and P(*h*CEMA-*r*-A), 0.51 mg, in $CDCl_3$ (c), and P(CEMA-*r*-T)-*b*-P*t*BA micelles containing P(*h*CEMA-*r*-A) in $CDCl_3/C_6D_{12}$ at v/v = 1/2.5 (d).

Table 1. Properties of the Diblock Used Determined in the PCEMA-*b*-P*t*BA Form

dn_r/dc^a (mL/g)	LS $\bar{M}_w{}^a$ (g/mol)	GPC^b $\bar{M}_w/\bar{M}_n$	NMR^a *n*/*m*	*n*
0.095	9.5 × 104	1.22	0.57	195

^{a} Measured in $CHCl_3$. ^{b} Measured in THF.

The precursor to P(CEMA-*r*-T)-*b*-P*t*BA was characterized in the PCEMA-*b*-P*t*BA form by GPC, NMR, and light scattering with results presented in Table 1. The diblock consisted of 195 HEMA and 340 *t*BA units. A ^{1}H NMR spectrum of P(CEMA-*r*-T)-*b*-P*t*BA is shown in Figure 1b. From the comparison between the intensities of the peaks at 11.4 ppm for thymine and at 6.7 ppm for cinnamoyl groups, a thymine labeling efficiency of 9% was obtained.

Formation of Micelles with Cores Containing P(hCEMA-*r*-A). Both the P*t*BA and P(CEMA-*r*-T) blocks dissolved in chloroform and only the P*t*BA block dissolved in CHX. The gradual addition of CHX into a P(CEMA-*r*-T)-*b*-P*t*BA solution in chloroform should lead to formation of micelles with P*t*BA coronas and P(CEMA-*r*-T) cores above a critical CHX content. This method of inducing micelle formation via addition of block selective solvents has been used extensively in the past[28] and should not introduce any surprises. Micelle formation could be qualitatively judged from the appearance of a bluish tint in the solution.

Table 2. Hydrodynamic and Electron Microscopic Diameters, D_h and D_E, and Polydispersity, K_2/K_1^2, of the Nanospheres at Different Stages in $C_6H_{12}/CHCl_3$ at v/v = 1/2.5

micelles			nanospheres			porous nanospheres		
D_h/nm	K_2/K_1^2	D_E/nm	D_h/nm	K_2/K_1^2	D_E/nm	D_h/nm	K_2/K_1^2	D_E/nm
61.4	0.027	22.7 ± 0.8	59.3	0.035	21.8 ± 1.0	60.7	0.017	22.6 ± 0.8

The more challenging aspect had been in demonstrating that P(hCEMA-*r*-A) was incorporated into the cores of the P(CEMA-*r*-T)-*b*-P*t*BA micelles during this process. The occurrence of this could be appreciated from several observations. First, the micellar solutions prepared following our method, involving equilibrating a chloroform solution of P(CEMA-*r*-T)-*b*-P*t*BA and P(hCEMA-*r*-A) overnight before CHX addition, were clear, bearing a bluish tint. If CHX was added immediately after the preparation of the chloroform solution, a slightly turbid solution bearing a bluish tint was prepared. Upon centrifugation, the turbidity disappeared, leaving a polymer precipitate at the bottom of the vial and a clear bluish solution at the top. This could be explained by the hypothesis that time was required for H bond formation and configuration reshuffling of the bonded chains as observed previously for another system.[29] If not enough time was allowed for H bonding between P(CEMA-*r*-T) and P(hCEMA-*r*-A) in chloroform, the addition of CHX would have led to formation of micelles with probably P(CEMA-*r*-T) cores. P(hCEMA-*r*-A), which has been shown by us insoluble in chloroform/CHX (1/2.5), would have precipitated out.

Shown in parts c and d of Figure 1 are the ^{1}H NMR spectra of a P(CEMA-*r*-T)-*b*-P*t*BA and P(hCEMA-*r*-A) mixture (w/w = 10/1.0) in $CDCl_3$ and in $CDCl_3/C_6D_{12}$ at v/v = 1.0/2.5, respectively. In $CDCl_3/C_6D_{12}$, the peaks of P(hCEMA-*r*-A) and P(CEMA-*r*-T) disappeared due to peak broadening or the slow motion of these chains. This provides convincing spectroscopic evidence for the formation of cores from P(CEMA-*r*-T) and P(hCEMA-*r*-A).

Micelle Cross-Linking. The micelles prepared were cross-linked with UV light that had passed a 290 nm cutoff filter to minimize light absorption by adenine. This was possible because the absorption maximum of adenine occurred at 260 nm, which was shorter than that of PCEMA at 274 nm. PCEMA cross-linking has been used extensively in our group in the past to facilitate the preparation of various block copolymer nanostructures.[30] PCEMA double bond conversion was obtained from absorbance decreases either in the UV region at 274 nm or in the infrared region at 1640 cm^{-1}. The effectiveness of the cross-linking reaction was judged from the stability of the cross-linked micelles in all kinds of solvents that solubilized both un-cross-linked PCEMA and P*t*BA.

Illustrated in Figure 2a is a TEM image of such cross-linked micelles. The cross-linked micelles were approximately spherical. Averaging over 50 particles yielded a TEM diameter D_E of 21.8 ± 1.0 nm. The hydrodynamic light scattering diameter D_h of the nanospheres was 59.3 nm. The D_h value is larger than the D_E value because D_h reflects the size of the nanospheres including the P*t*BA coronas in a solvated state and D_E is a measure for the size of the cores of the dry particles.

Similar TEM images were obtained for the micelles before crosslinking. The D_E and D_h values for the micelles were 22.7 ± 0.8 and 61.4 nm, respectively. These numbers agree well with those reported for the cross-linked micelles or nanospheres. This size invariance of the micelles with cross-linking has been demonstrated by us before[31] and suggests insignificant perturbation of micellar structures by cross-linking.

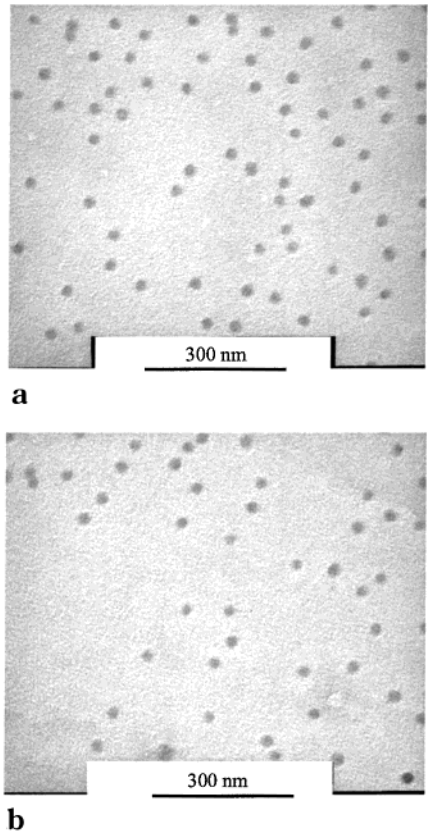

Figure 2. TEM images of P(CEMA-*r*-T)-*b*-P*t*BA nanospheres containing P(*h*CEMA-*r*-A) (a) and P(CEMA-*r*-T)-*b*-P*t*BA porous nanospheres (b).

Porogen Extraction. Removal of P(hCEMA-*r*-A) from the cores of the nanospheres was confirmed from gravimmetric and NMR analyses. As mentioned in the Experimental Section, the porogen recovery efficiency from DMF extraction after nanosphere cross-linking was 90%. A NMR analysis revealed an insignificant change in the spectrum of the extracted porogen and thus suggested minimal radiation damage to it. Illustrated in Figure 2b is a TEM image of the porous nanospheres. The TEM diameter D_E averaged over 50 spheres and D_h are 22.8 ± 0.8 and 60.7 nm, respectively, which agree well with 21.8 ± 1.0 and 59.3 nm for the spheres before porogen extraction. The invariance in the D_E and D_h values with porogen extraction suggests that the spheres did not shrink after porogen removal and the preparation of nanospheres with porous cores.

Adenine Uptake. Adenine and thymine are two of the constituent and complementary bases of DNA and form two H bonds with each other. The porous nanospheres with thymine groups in the cores should uptake adenine. A challenge had been in developing a method to monitor the kinetics of this process. Traditionally, a downfield shift in the thymine imino resonance at ~11 ppm had been used to quantify T−A paring.[32] The difficulty here was that the NMR signals of thymine

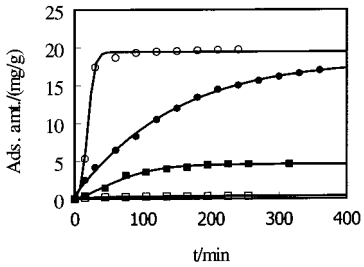

Figure 3. Kinetic data of adenine uptake by the P(CEMA-*r*-T)-*b*-P*t*BA porous nanospheres (○), P(CEMA-*r*-T)-*b*-P*t*BA solid nanospheres (●), and PCEMA-*b*-P*t*BA nanospheres (■). Also shown for comparison are the data from the control experiment where no nanospheres were used (□).

groups were not visible due to their location inside the cores. We could have monitored adenine concentration variation in the supernatant as a function of time of equilibration between the nanospheres and adenine after nanosphere separation by ultracentrifugation, if we had access to such a centrifuge. Without an ultracentrifuge, we hydrolyzed the *tert*-butyl groups off the P*t*BA coronas to produce poly(acrylic acid) coronal chains. After adenine uptake from water, the nanospheres were separated from the supernatant by adding $CaCl_2$ to induce nanosphere settling.[33] The nanospheres did not settle completely this way, and a trace amount of nanospheres left behind interfered with UV absorbance analysis of adenine content.

We eventually circumvented the difficulty by equilibrating a nanosphere solution in methanol trapped inside a dialysis tube with an adenine solution outside. The large nanospheres could not pass the membrane and adenine concentration decreased outside because of their ability to pass the membrane and be sorbed by the nanospheres. The complication here was that the external adenine concentration decreased also due to membrane sorption and dilution of the external solution by the liquid inside the dialysis tube. This dilution effect could, in principle, be minimized from using an excess of solution outside the tube. We used the solution volumes of 100.0 and 5.00 mL outside and inside the tube, respectively. We also monitored the combined effect of dilution and membrane sorption experimentally. In this case, we inserted a dialysis tube containing 5.0 mL of neat methanol into an adenine solution and then followed the change in external adenine concentration, $c(t)$, as a function of time. The amount of adenine, $\Delta m(t)$, disappearing at time t was calculated using

$$\Delta m(t) = m(0)\frac{c(0) - c(t)}{c(0)} \tag{1}$$

where $m(0)$ and $c(0)$ were the total adenine mass and initial concentration outside the tube, respectively. To facilitate comparison with data of adenine sorption by nanospheres, we artificially divided $\Delta m(t)$ from the control experiment by the amount of nanospheres, 5.0 mg, used in all sorption experiments. The data were presented in terms of milligrams of adenine sorbed by each gram of spheres, $\Delta m'(t)$ or a fictitious specific sorbed amount, in Figure 3.

Data for adenine sorption by the porous and solid P(CEMA-*r*-T)-*b*-P*t*BA nanospheres and the PCEMA-*b*-P*t*BA nanospheres were obtained similarly. A glimpse of Figure 3 revealed that the adenine sorption amounts from the control experiment were insignificant relative to those obtained from other runs. For this and for the fact that we did not know how to correct for the membrane sorption and solution dilution effect properly, the raw sorption data were presented without correction in Figure 3.

One feature of Figure 3 was that the porous spheres sorbed adenine much faster than the other spheres. Because of the unconventional experimental design, it was difficult to treat the sorption data with classical ion-exchange resin sorption models.[34] The curves were thus drawn through the data points only for visual aids and did not represent best fits from equations with any physical significance. Regardless of the mechanistic details of adenine sorption, the fact that the porous nanospheres uptook adenine with a much higher rate than the others under identical conditions represented compelling evidence for the presence of pores in such cores.

Unfortunately, the solid nanospheres were able to uptake just as much adenine, i.e., at ~20 mg/g, as the porous ones at sorption equilibrium. This was probably caused by the small size of adenine and its facilitated penetration into the cores of both the solid and porous P(CEMA-*r*-T)-*b*-P*t*BA nanospheres.

Thymine−Adenine Binding Constant. Since the dialysis membrane sorbed adenine insignificantly, the sorption equilibrium data could be treated to estimate the T−A binding constant. By definition, the apparent constant of binding between thymine and adenine was

$$K_{ab} = \frac{[AT]_N}{[T]_N[A]_{OH}} \tag{2}$$

where $[AT]_N$ and $[T]_N$ denote the A−T complex and free T group concentrations at sorption equilibrium in the nanosphere cores, respectively, and $[A]_{OH}$ is the equilibrium adenine concentration in bulk methanol. $[AT]_N$ and $[T]_N$ are obtained from dividing the mole numbers n_{AT} and n_T for A−T and T by the nanosphere core volume. Canceling the nanosphere core volume term in the numerator and denominator of eq 2 yields

$$K_{ab} = \frac{n_{AT}}{n_T[A]_{OH}} \tag{3}$$

To estimate n_{AT}, we assumed unrealistically that all of the sorbed adenine formed 1:1 complex with the T groups. On the basis of this assumption and the equilibrium sorption amount of ~20 mg/g, n_{AT} in 5.0 mg of nanospheres was calculated to be $\sim 7.4 \times 10^{-7}$ mol. The free T groups in 5.0 mg of the nanospheres after adenine binding was $\sim 1.9 \times 10^{-7}$ mol. The concentration of adenine in methanol was 9.2×10^{-6} M. Inserting these numbers into eq 3 we obtained $K_{ab} = 4.2 \times 10^5\ M^{-1}$.

The value $4.2 \times 10^5\ M^{-1}$ represented an upper bound for K_{ab}, and it should decrease somewhat after correcting for the fact that not all of the sorbed adenine participated in the T−A pairing. This K_{ab} value is far greater than the association constant K_{as} of ~40 M^{-1} reported for thymine and adenine in chloroform.[35,36] The K_{ab} value is much larger as it is different from K_{as}. In fact, K_{ab} is[32]

$$K_{ab} = \frac{[AT]_N}{[T]_N[A]_N}\frac{[A]_N}{[A]_{OH}} = K_{as}K_p \tag{4}$$

where $[A]_N$ denotes the equilibrium concentration of adenine, in the nanosphere cores, that was not bound

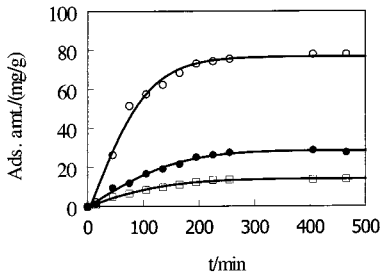

Figure 4. Kinetic data of P(*h*CEMA-*r*-A) uptake by the P(CEMA-*r*-T)-*b*-P*t*BA porous (○) and solid (●) nanospheres. Also shown for comparison are the data from the control experiment where no nanospheres were used (□).

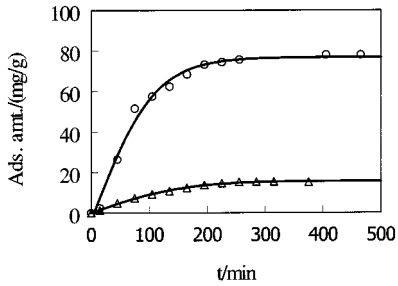

Figure 5. Comparison between the kinetic data of P(*h*CEMA-*r*-A) (○) and PCEMA (△) uptake by the P(CEMA-*r*-T)-*b*-P*t*BA porous nanospheres. The data were not corrected for oligomer adsorption by the dialysis membrane.

to thymine and K_p is the coefficient of partition of unbound adenine between the nanosphere cores and methanol.

The partition coefficient is the ratio between the equilibrium concentrations of unbound adenine in the P(CEMA-*r*-T)-*b*-P*t*BA cores and in methanol. This coefficient can be approximately estimated from the data of equilibrium adenine uptake by PCEMA-*b*-P*t*BA nanospheres, where all of the sorbed adenine molecules are not bound to thymine groups. Assuming insignificant swelling of the core by methanol and using a density of 1.25 g/mL for PCEMA,[37] we estimated a core volume of 2.1×10^{-3} mL for 5.0 mg of the PCEMA-*b*-P*t*BA nanospohere. The equilibrium adenine uptake density of 4.6 mg/g shown in Figure 3 corresponded to 1.70×10^{-7} mol of adenine in 5.0 mg of nanospheres. The equilibrium concentration of adenine in methanol was 1.46×10^{-5} M. Ratioing the molar concentrations of adenine in the nanosphere cores and methanol, we obtained $K_p = 5.5 \times 10^3$. Inserting the K_p value into eq 4 yielded $K_{as} = 76\ M^{-1}$. The K_{as} value is now close to but still larger than the value determined for T−A binding in chloroform. The discrepancy was most likely caused by the assumption that all of the sorbed adenine formed 1:1 complex with thymine in the P(CEMA-*r*-T)-*b*-P*t*BA nanosphere cores.

The K_p value of 5.5×10^3 surprised us initially, because the K_p value for adenine partition between water and low-molar mass surfactant micelle cores is typically between 10 and 100.[36] This large K_p value is reasonable, however. K_p is low for adenine partition between water and surfactant cores, because adenine was shown by us to be slightly soluble both in water and in hexane, and hexane may have similar solubilization characteristics for adenine as the surfactant micelle cores. K_p is much larger in our case, because the solubility of adenine is low only in methanol but high in DMF. We expect adenine to have similar solubility in the PCEMA cores as in DMF, because chloroform was shown to swell cross-linked PCEMA gel pronouncedly.

P(hCEMA-*r*-A) Uptake. At sorption equilibrium, the porous and solid P(CEMA-*r*-T)-*b*-P*t*BA nanospheres sorbed an equal amount of adenine from methanol. We wondered if the uptake selectivity of the porous nanospheres could be improved if the porogen or the "template" was used as the adsorbate. Illustrated in Figure 4 was the comparison between the kinetic data of P(hCEMA-*r*-A) uptake in chloroform by the porous and solid P(CEMA-*r*-T)-*b*-P*t*BA nanospheres. Also presented were data obtained from a control experiment where no nanospheres were used.

First, we note that the porous nanospheres picked up P(hCEMA-*r*-A) again faster. Second, much higher relative readings were obtained from the control experiment than those shown in Figure 3. This was probably caused by P(hCEMA-*r*-A) trapping or sorption in the membrane pores. Third, the amount of P(hCEMA-*r*-A) picked up by the porous nanospheres at equilibrium was much higher than that of the solid nanospheres or the selectivity of the porous nanospheres indeed increased. Subtracting the leveled amount of 13.9 mg/g of the control experiment from the equilibrium specific sorbed amounts of 78 and 28.2 mg/g, we obtained the corrected equilibrium specific uptake amounts of 64 and 14.3 mg/g for the porous and nonporous nanospheres. This corresponded to a selectivity of 5/1 for the porous relative to the solid nanospheres. The much-improved selectivity here confirms once again the presence of cavities inside the cores of the porous nanospheres. The specific sorbed amount of 64 mg/g for the porous nanospheres was close to 87 mg of porogen extracted from each gram of nanospheres and suggested a high degree of utilization of the cavities. The solid nanospheres picked up P(hCEMA-*r*-A) probably due to their deposition on the surfaces of the nanosphere cores via T−A binding.

PCEMA Chain Uptake. The selectivity of the porous over nonporous P(CEMA-*r*-T)-*b*-P*t*BA nanospheres for P(hCEMA-*r*-A) suggested our success in molecularly "imprinting" nanometer-sized solvent-dispersible spheres. Molecularly imprinted cavities recognize their templates or analogues supposedly not only based on size fit or size recognition but also on functional binding or functionality recognition.[2] Since the P(hCEMA-*r*-A) porogen used here had a molar mass distribution, the meaning of size recognition should be adjusted accordingly. A P(hCEMA-*r*-A) sample with a significantly higher $\bar{M}_n$ than that of the porogen may still be sorbed by the porous spheres, because its molar mass distribution may overlap with that of the porogen used. To limit the scope of this paper, we will not dwell further on testing the size recognition capability of the porous nanospheres. We will, however, show that adenine groups are essential in ensuring adsorbate uptake.

To show this, we tried to compare the kinetics of P(hCEMA-*r*-A) and PhCEMA uptake by the porous nanospheres. Such an experiment, however, failed to deliver quick results because PhCEMA did not absorb significantly above 254 nm. Below 254 nm, chloroform absorbed significantly and interfered with the UV absorbance analysis. CEMA differed from hCEMA only in the hydrogenation of the aliphatic double bond and we expected little size change by replacing PhCEMA with PCEMA. The use of PCEMA significantly simplified the experimental procedures as PCEMA absorbed strongly at 274 nm.

Shown in Figure 5 is the comparison between the kinetic data of PCEMA and P(hCEMA-*r*-A) sorption by the porous nanospheres. The absolute values should be flawed as before due to membrane sorption. In fact, the data of PCEMA sorption match those of the control experiment shown in Figure 4 closely. Thus, the porous nanospheres sorbed PCEMA chains negligibly, despite the size match between PCEMA and P(hCEMA-*r*-A).

IV. Conclusions

We have prepared and characterized P(CEMA-*r*-T)-*b*-P*t*BA and P(hCEMA-*r*-A). The two polymers were dissolved in chloroform and the addition of CHX to the volume fraction of 71% lead to micelle formation consisting of P*t*BA coronas and P(CEMA-*r*-T) and P(hCEMA-*r*-A) cores. Pores were generated in the cores after photo-cross-linking the cores and extracting out the porogen with DMF. The presence of pores in the cores of the porous nanospheres was demonstrated by their much faster uptake of adenine from methanol and P(hCEMA-*r*-A) from chloroform than the solid P(CEMA-*r*-T)-*b*-P*t*BA nanospheres. This was also confirmed by the much higher uptaking capacity of the porous nanospheres for P(hCEMA-*r*-A). The porous nanospheres were shown to have functionality recognition capability, as they did not uptake PCEMA chains. The nanospheres exhibited extraordinarily high apparent constant for adenine binding in methanol because of favorable partition of adenine inside the nanosphere cores.

One should be able to generalize the method used here to prepare porous spheres containing various binding groups. The porous spheres thus produced should be useful as microextractor that can extract or preconcentrate analyte of interest selectively from a mixture for further analysis and quantification.[38] One can also cleave the *tert*-butyl groups off the P*t*BA coronal chains and prepare water-dispersible porous nanospheres.[15] Such nanospheres containing porous cores and thymine groups on the cavity walls should bind adenine even in aqueous environments.[32,39,40]

Acknowledgment. NSERC of Canada is gratefully acknowledged for sponsoring this research. Dr. X. Yan is thanked for preparing Scheme 1.

References and Notes

(1) For reviews on this subject, see, for example: (a) Seidl, J.; Malinsky, J.; Dusek, K.; Heitz, W. *Adv. Polym. Sci.* **1967**, *5*, 113. (b) Guyot, A.; Bartholin, M. *Prog. Polym. Sci.* **1982**, *8*, 277.
(2) (a) Wulff, G. *Angew. Chem., Int. Ed. Engl.* **1995**, *34*, 1812. (b) Steinke, J.; Sherrington, D. C.; Dunkin, I. R. *Adv. Polym. Sci.* **1995**, *123*, 81. (c) Shea, K. J. *Trends Polym. Sci* **1994**, *2*, 166. (d) Sellergren, B. *Angew. Chem., Int. Ed.* **2000**, *39*, 1032.
(3) Wulff, G.; Poll, H.-G. *Makromol. Chem.* **1987**, *188*, 741.
(4) Spivak, D. A.; Shea, K. J. *Macromolecules* **1998**, *31*, 2160.
(5) Asanuma, H.; Hishiya, T.; Ban, T.; Gotoh, S.; Komiyama, M. *J. Chem. Soc., Perkin Trans. 2,* **1998** 1915.
(6) Yoshida, M.; Hatate, Y.; Uezu, K.; Goto, M.; Furusaki, S. *J. Polym. Sci.: A: Polym Chem.* **2000**, *38*, 689.
(7) Sellergren, B.; Ekberg, B.; Mosbach, K. *J. Chromatogr.* **1985**, *347*, 1.
(8) Sellergren, B. *Angew. Chem., Int. Ed.* **2000**, *39*, 1031.
(9) Ugelstad, J.; Kaggerud, K. H.; Hansen, F. K.; Berger, A. *Makromol. Chem.* **1979**, *180*, 737.
(10) Wang, Q. C.; Švec, F.; Fréchet, M. J. *J. Polym. Sci., A: Polym. Chem.* **1994**, *32*, 2577.
(11) Ye, L.; Mosbach, K. *J. Am. Chem. Soc.* **2001**, *123*, 2901.
(12) Švec, F.; Fréchet, M. J. *Anal. Chem.* **1992**, *64*, 820.
(13) Matsui, J.; Kato, T.; Takeuchi, T.; Suzuki, M.; Yokoyama, K.; Tamiya, E.; Karube, I. *Anal. Chem.* **1993**, *65*, 2223.
(14) Wang, M.; Zhang, G. Z.; Chen, D. Y.; Jiang, M.; Liu, S. Y. *Macromolecules* **2001**, *34*, 7172.
(15) Henselwood, F.; Liu, G. J. *Macromolecules* **1998**, *31*, 4213.
(16) (a) Zhang, L.; Eisenberg, A. *Science* **1995**, *268*, 1728. (b) Zhang, L.; Yu, K.; Eisenberg, A. *Science* **1996**, *272*, 1777.
(17) (a) Ding, J.; Liu, G. *Macromolecules* **1997**, *30*, 2408. (b) Ding, J.; Liu, G.; Yang, M. *Polymer* **1997**, *38*, 5497.
(18) Jenekhe, S. A.; Chen, X. L. *Science* **1998**, *279*, 1903.
(19) Discher, B. M.; Won, Y. Y.; Ege, D. S.; Lee, J. C−M.; Bates, F. S.; Discher, D. E.; Hammer, D. A. *Science* **1999**, *284*, 1143.
(20) (a) Ding, J.; Liu, G. J. *J. Phys. Chem. B.* **1998**, *102*, 6107. (b) Ding, J.; Liu, G. J. *Chem. Mater.* **1998**, *10*, 537.
(21) (a) Underhill, R. S.; Liu, G. J. *Chem. Mater.* **2000**, *12*, 2082. (b) Stewart, S.; Liu, G. J. *Chem. Mater.* **1999**, *11*, 1048. c) Underhill, R. S.; Liu, G. J. *Chem. Mater.* **2000**, *12*, 3633.
(22) Liu, G.; Ding, J.; Hashimoto, T.; Saijo, K.; Winnik, F. M.; Nigam, S. *Chem. Mater.* **1999**, *11*, 2233.
(23) Guo, A.; Tao, J.; Liu, G. J. *Macromolecules* **1996**, *29***,** 2487.
(24) Hassner, A.; Alexanjan, V. *Tetrah. Lett.* **1978**, *46*, 4475.
(25) Thomson, S. A.; Josey, J. A.; Cadilla, R.; Gaul, M. D.; Hassman, F.; Luzzio, M. J.; Pipe, A. J.; Reed, K. L.; Ricca, D. J.; Eiethe, R. W.; Noble, S. A. *Tetrahedron* **1995**, *51*, 6179.
(26) Holmberg, K.; Hansen, B. *Acta Chem. Scand.* **1979**, *B33*, 410.
(27) Ding, J.; Liu, G. J. *Macromolecules* **1999**, *32*, 8413.
(28) See, for example: (a) Tuzar, Z.; Kratochvil, P. *Surf. Colloid Sci.* **1992**, *15*, 1. (b) Cameron, N. S.; Corbierre, M. K.; Eisenberg, A. *Can. J. Chem.* **1999**, *77*, 1311. (c) Ding, J.; Liu, G. J.; Yang, M. *Polymer* **1997**, *38*, 5497.
(29) Cusack, L.; Rizza, R.; Corelov, A.; Fitzmaurice, D. *Angew. Chem., Int. Ed.* **1997**, *36*, 8484.
(30) Liu, G. J. *Curr. Opin. Colloid Interface Sci.* **1998**, *3*, 200.
(31) Tao, J.; Stewart, S.; Liu, G. J.; Yang, M. *Macromolecules* **1997**, *30*, 2738.
(32) Nowick, J. S.; Chen, J. S.; Noronha, G. *J. Am. Chem. Soc.* **1993**, *115*, 7636.
(33) (a) Henselwood, F.; Liu, G. J. *Macromolecules* **1997**, *30*, 488. (b) Wang, G.; Henselwood, F.; Liu, G. J. *Langmuir* **1998**, *14*, 1554.
(34) See, for example: Grimshaw, R. W.; Harland, C. E. *Ion Exchange: Introduction to Theory and Practice*: Chemical Society Press: London, 1975.
(35) Sirish, M.; Maiya, B. G. *J. Porphyrins Phthalocyanines* **1998**, *2*, 327.
(36) Nowick, J. S.; Cao, T.; Noronha, G. *J. Am. Chem. Soc.* **1994**, *116*, 3285.
(37) (a) Liu, G. J.; Ding, J.; Hashimoto, T.; Saijo, K.; Winnik, F. M.; Nigam, S. *Chem. Mater.* **1999**, *11*, 2233. (b) Liu, G. J.; Ding, J.; Qiao, L.; Guo, A.; Gleeson, J. T.; Dymov, B.; Hashimoto, T.; Saijo, K. *Chem.−Eur. J.* **1999**, *5*, 2740.
(38) Li, S.; Sun, L. F.; Chung, Y. S.; Weber, S. G. *Anal. Chem.* **1999**, *71*, 2146.
(39) Torneiro, M.; Still, C. *J. Am. Chem. Soc.* **1995**, *117*, 5887.
(40) Totello, V. M.; Viani, E. A.; Deslongchamps, G.; Murray, B. A.; Rebek Jr. J. *J. Am. Chem. Soc.* **1993**, *115*, 797.

MA0120005